NeuroImage: Clinical 30 (2021) 102680

Contents lists available at ScienceDirect

NeuroImage: Clinical

journal homepage: www.elsevier.com/locate/ynicl

Cervical and thoracic cord atrophy in multiple sclerosis phenotypes: Quantification and correlation with clinical disability

Yair Mina [a,b,1], Shila Azodi [a,c,1], Tsemacha Dubuche [a], Frances Andrada [c], Ikesinachi Osuorah [c], Joan Ohayon [c], Irene Cortese [c], Tianxia Wu [d], Kory R. Johnson [e], Daniel S. Reich [f], Govind Nair [c,g], Steven Jacobson [a,*]

[a] Viral Immunology Section, National Institute of Neurological Disorders and Stroke, National Institutes of Health, Bethesda, MD, United States
[b] Sackler Faculty of Medicine, Tel-Aviv University, Tel-Aviv, Israel
[c] Neuroimmunology Clinic, National Institute of Neurological Disorders and Stroke, National Institutes of Health, Bethesda, MD, United States
[d] Clinical Trials Unit, National Institute of Neurological Disorders and Stroke, National Institutes of Health, Bethesda, MD, United States
[e] Bioinformatics Section, National Institute of Neurological Disorders and Stroke, National Institutes of Health, Bethesda, MD, United States
[f] Translational Neuroradiology Section, National Institute of Neurological Disorders and Stroke, National Institutes of Health, Bethesda, MD, United States
[g] Quantitative MRI Core Facility, National Institute of Neurological Disorders and Stroke, National Institutes of Health, Bethesda, MD, United States

ARTICLE INFO

Keywords:
Multiple Sclerosis
Spine
MRI

ABSTRACT

Objective: We sought to characterize spinal cord atrophy along the entire spinal cord in the major multiple sclerosis (MS) phenotypes, and evaluate its correlation with clinical disability.

Methods: Axial T_1-weighted images were automatically reformatted at each point along the cord. Spinal cord cross-sectional area (SCCSA) were calculated from C1-T10 vertebral body levels and profile plots were compared across phenotypes. Average values from C2-3, C4-5, and T4-9 regions were compared across phenotypes and correlated with clinical scores, and then categorized as atrophic/normal based on z-scores derived from controls, to compare clinical scores between subgroups. In a subset of relapsing-remitting cases with longitudinal scans these regions were compared to change in clinical scores.

Results: The cross-sectional study consisted of 149 adults diagnosed with relapsing-remitting MS (RRMS), 49 with secondary-progressive MS (SPMS), 58 with primary-progressive MS (PPMS) and 48 controls. The longitudinal study included 78 RRMS cases. Compared to controls, all MS groups had smaller average regions except RRMS in T4-9 region. In all MS groups, SCCSA from all regions, particularly the cervical cord, correlated with most clinical measures. In the RRMS cohort, 22% of cases had at least one atrophic region, whereas in progressive MS the rate was almost 70%. Longitudinal analysis showed correlation between clinical disability and cervical cord thinning.

Conclusions: Spinal cord atrophy was prevalent across MS phenotypes, with regional measures from the RRMS cohort and the progressive cohort, including SPMS and PPMS, being correlated with disability. Longitudinal changes in the spinal cord were documented in RRMS cases, making it a potential marker for disease progression. While cervical SCCSA correlated with most disability and progression measures, inclusion of thoracic measurements improved this correlation and allowed for better subgrouping of spinal cord phenotypes. Cord atrophy is an important and easily obtainable imaging marker of clinical and sub-clinical progression in all MS phenotypes, and such measures can play a key role in patient selection for clinical trials.

1. Introduction

Multiple sclerosis (MS) is a chronic inflammatory demyelinating disease of the central nervous system and is a leading cause of disability in young adults. (Longo et al., 2018) Individuals with the disease are categorized into clinical phenotypes including relapsing-remitting MS (RRMS), secondary progressive MS (SPMS), and primary progressive MS (PPMS). (Lublin et al., 2014) While radiological analysis of the brain in MS has been extensively studied, (Sastre-Garriga et al., 2020) relatively less information is available regarding the spinal cord, especially the

* Corresponding author.
E-mail address: jacobsons@nih.gov (S. Jacobson).
[1] These authors contributed equally to the manuscript.

https://doi.org/10.1016/j.nicl.2021.102680
Received 19 November 2020; Received in revised form 15 April 2021; Accepted 16 April 2021
Available online 28 April 2021

thoracic spinal cord, even though it is evidently involved in the disease process. (Losseff et al., 1996; Horsfield and Filippi, 2003; Moccia et al., 2019; Zurawski et al., 2019; Casserly et al., 2018; Bot et al., 2004; Azodi et al., 2017; Ciccarelli et al., 2019) Accumulating evidence supports routine measurement of cervical spine (C-spine) area loss in MS, as well as further research to establish the role of spinal cord atrophy in treatment monitoring, as was evident in a recent consensus statement from the Magnetic Resonance Imaging in MS study group. (Sastre-Garriga et al., 2020)

Spinal cord atrophy, especially investigated in the C-spine, is a common phenomenon in the disease, especially in its progressive phenotypes. (Bot et al., 2004; Azodi et al., 2017). It has been shown to correlate with clinical disability (Bonati et al., 2011; Bjartmar et al., 2000; Song et al., 2020; Daams et al., 2015; Cohen et al., 2012; Ukkonen et al., 2003; Oh et al., 2015) independent of other imaging measurements, (Daams et al., 2015; Cohen et al., 2012; Oh et al., 2015; Andelova et al., 2019) and is a possible marker of disease progression when measured longitudinally. (Aymerich et al., 2018; Tsagkas et al., 2018; Lukas et al., 2015; Stevenson et al., 1998) Furthermore, clinical correlation with cord atrophy has been shown to be stronger than with spinal cord lesion load. (Cohen et al., 2012) However, spinal cord atrophy studies comparing different MS phenotypes (Tsagkas et al., 2018; Bernitsas et al., 2015; Rocca et al., 2019, 2011; Bieniek et al., 2006) are few, and studies involving thoracic spine (T-spine) (Ukkonen et al., 2003; Schlaeger et al., 2015; Klein et al., 2011) are even fewer.

Being a promising imaging marker, some clinical trials in MS have tried using C-spine atrophy measurements as outcomes (Leary et al., 2003; Lin et al., 2003; Kapoor et al., 2010; Tur et al., 2018), but results were disappointing and inconclusive, possibly in part due to the challenges in reproducibility of methods. These challenges, are reflected in some previous studies on cord atrophy (Stevenson et al., 1998; Bernitsas et al., 2015; Schlaeger et al., 2015) which were based on spinal cord cross-sectional area (SCCSA) on axial slice(s) placed on specific levels of the spinal cord, and these were addressed to some degree by newer methods using volumetric imaging and mathematical modeling for calculation of SCCSA (Daams et al., 2014; De Leener et al., 2017; Liu et al., 2014) or other surrogates of longitudinal changes. (Prados et al., 2020) To overcome these issues, recent years have seen a proliferation of methods for quantifying spinal cord atrophy. Several groups have used volumetric imaging and mathematical modeling as well as deep learning to determine the cross-sectional area in upper-cervical, entire cervical spinal cord, or the whole spinal cord (De Leener et al., 2017; Liu et al., 2014; McCoy et al., 2019).

We have previously reported a robust automated approach to obtaining SCCSA perpendicular to the spinal cord at every point along the C- and T-spine, and we have applied this approach in neuroinflammatory diseases including human T-lymphocytic virus 1 (HTLV-1) associated myelopathy and MS. (Azodi et al., 2017) Our prior studies showed differences across MS phenotypes, as adults with progressive MS phenotypes — SPMS and PPMS — had on average a thinner cervical cord compared to RRMS. Here, we extend these observations to a larger MS population, with the aims of: (1) characterizing SCCSA profile in different MS phenotypes and exploring their clinical correlations; (2) performing subgroup analysis of regional-SCCSA to better understand atrophy patterns and clinical progression; and (3) evaluating longitudinal changes in regional-SCCSA and their implications for clinical progression.

2. Materials and methods

2.1. Study design

Adults clinically diagnosed with MS and healthy control participants (HC) were recruited into natural history studies approved by the institutional review board of the National Institutes of Health (Clinical Trials identifier NCT00001248 and NCT00001778) after informed consent. All participants underwent a detailed clinical and neurological examination, and MS cases were diagnosed and categorized into RRMS, SPMS, and PPMS phenotypes. (Lublin et al., 2014) Clinical disability scales measured on all MS cases included expanded disability status scale (EDSS), Scripps neurologic rating scale (SNRS), timed 25-foot walk (T25FW) and 9-hole peg test (9-HPT). T25FW and 9-HPT were also obtained on HC.

Participants underwent MRI scan of the C-spine and T-spine on a Siemens 3-tesla scanner (Siemens Healthcare GmbH, Erlangen, Germany), equipped with a 24-channel head-and-neck coil or a 32-channel head coil with 24-channel spine matrix coil which included T_1-weighted scans of the spinal cord (3D gradient recalled echo sequence, repetition time = 8 ms, echo time = 3 ms, flip angle = 18 degrees, 1-mm isotropic resolution, total acquisition time of about 3.5 min each for C- and T-spine).

SCCSA was calculated from these MRI images, the detailed procedure for which was given previously. (Liu et al., 2014) In this technique, 3D T_1-weighted images from C-spine and T-spine were stitched together using table position information on the DICOM headers. Next, location of spinal cord edges from vertebral levels C1 and T10 was manually selected on the stitched sagittal image of the spinal cord using scripts written in Matlab (The MathWorks, Inc., Natick, MA). Axial images perpendicular to the edge were automatically reformatted at each point along the selected spinal cord edge. The user then has an opportunity to check the goodness of the edges automatically detected on the spinal cord. Once the entire cord segmentation passes the manual quality-assurance step, a second pass for cross-sectional area is made, but this time using the geometric center of the segmented cord and cross-sectional area at each point along the cord calculated and plotted against normalized distance from C1-T10. SCCSA profile plots for individuals are displayed with HC and SPMS group averages for reference. The thickness of the band in the plot depicts mean ± 1 standard error of the mean of each group. Reliability of the measure has been reported previously. (Liu et al., 2014) In addition, for statistical comparisons, average SCCSA were derived from specific regions (regional-SCCSA) including: C2-C3 (a region containing predominantly white matter tracts that is commonly used in longitudinal MS studies[22]); C4-C5 (corresponding to the cervical enlargement and including substantially more gray matter than the C2–C3 region); and T4 to T9 (mostly white matter tracts related to the lower extremities). The region of C6 to T3 was excluded because normal anatomical variation in this area where the slope of SCCSA change is steep, caused large variance in regional measurements, which in turn makes it difficult to detect differences between groups.

2.2. Statistical analysis

Statistical analyses were performed with SAS (v9.4). Differences in age and sex between groups were evaluated using a one-way ANOVA followed by Tukey's multiple comparisons test. Regional-SCCSA variables, adjusted for sex effect (estimated from HC), were used for statistical analysis. SCCSA measures did not correlate with age of participant in the HC, and regional-SCCSA in MS patients did not correlate with age when controlled for disease duration. Therefore, adjustment for age was not performed in the analysis. To examine the difference in regional-SCCSA between groups (RRMS, PPMS, SPMS, HC), a one-way ANOVA was performed, followed by Tukey's multiple comparisons test. A p-value of <0.0167, adjusting for multiple comparisons (three regions), was considered statistically significant.

The Box-Cox transformation was applied to the clinical parameter variables. The Shapiro-Wilk test was applied to examine the normality of the model residuals. Pearson correlation coefficients were used to examine association between transformed clinical parameters and SCCSA variables in two cohorts (RRMS and the combined progressive cohort). To adjust for multiple comparisons (three regions, two groups, five clinical parameters), a p-value of <0.0017 was considered

Table 1
Participant demographics and clinical characteristics – Demographics and clinical scores of (A) cross-sectional cohorts and (B) longitudinal RRMS cohort, which was divided into those showing progressive-disability (EDSS change ≥ 1 for baseline EDSS ≤ 5.5 and EDSS change ≥ 0.5 for baseline EDSS ≥ 6) and those with stable-disability (all others).

A. Cross-sectional Study								
Diagnosis	N (% female)	Age (y, mean ± SD)	DD (y, med., IQR)	EDSS (med., IQR)	SNRS (mean ± SD)		T25FW (s, med., IQR)	9HPT-A (s, med., IQR)
HC	48 (55%)	45 ± 14	N/A	N/A	N/A		4 (3–6)	18 (14–23)
RRMS	149 (70%)	44 ± 12	7 (2–15)	1.5 (1–2)	90 ± 10		5 (4–5)	19 (17–21)
SPMS	49 (65%)	55 ± 11[b]	24 (14–30)	6.5 (6–6.5)	64 ± 14		10 (6–16)	28 (23–36)
PPMS	59 (47%)[a]	54 ± 11[b]	11 (7–16)	6 (5–6.5)	65 ± 13		7 (5–13)	29 (22–34)
B. Longitudinal Study								
Group	Time Point	N(% female)	FI (y,med., IQR)	Age (y, mean ± SD)	DD (y, med., IQR)	EDSS (med., IQR)	SNRS(mean ± SD)	T25FW (s, med., IQR)	9HPT-A (s, med., IQR)
Entire Cohort	Baseline	78 (55%)		42 ± 12	4 (2–11)	1.5 (1–2)	93 ± 7	4.7 (4.1–5.1)	18 (17–21)
	Follow up		1.5 (1–2.2)	44 ± 12	7 (4–12)	1.5 (1–2)	92 ± 10	4.8 (4.3–5.5)	18 (16–21)
Stable-disability group	Baseline	64 (55%)		42 ± 12	5 (2–11)	1.5 (1–1.5)	94 ± 6	4.5 (4–4.9)	18 (17–21)
	Follow up		1.3 (1–2.1)	44 ± 12	7 (4–12)	1.5 (1–1.5)	94 ± 7	4.7 (4.2–5.3)	18 (16–20)
Progressive-disability group	Baseline	14 (57%)		42 ± 10	3 (2–7)	1 (0–2)	93 ± 9	4.7 (4.4–5.8)	18 (17–20)
	Follow up		1.7 (1.4–2.1)	44 ± 11	5 (3–10)	2 (1–5)[c]	82 ± 13[c]	5.6 (4.7–7.2)	19 (18–24)[c]

9-HPT-A – time to complete 9-hole peg test (average of left and right), DD – disease duration, EDSS – expanded disability status scale, FI – follow-up interval, HC – healthy controls, IQR – inter-quartile range (reported as quartile 1, quartile 3), med. – median, N/A – not applicable, PPMS – primary progressive multiple sclerosis, RRMS – relapsing remitting multiple sclerosis, s – seconds, SNRS – Scripps neurologic rating scale, SPMS – secondary progressive multiple sclerosis, T25FW – timed 25-foot walk, , y – years.

[a] Significantly different from RRMS group ($p = 0.002$).
[b] Significantly different from RRMS and HC groups ($p < 0.001$).
[c] Significantly different from stable-disability group at follow up ($p < 0.05$)

statistically significant.

Following evaluation of association between SCCSA measurements in the different regions using Pearson correlation coefficients, a backward elimination regression analysis was implemented to assess for the relative effect of each region on each clinical parameter in the two cohorts (RRMS and the combined progressive cohort). For each parameter in each group, a model including all 3 regions was created, in which regions with a non-significant impact (p-value ≥ 0.10) were removed, until no further regions could be removed without a statistically significant loss of the model fit.

RRMS, SPMS, and PPMS groups were further divided into four subgroups based on regional-SCCSA using z-score (mean and standard deviation estimated from HC group) of −1.64 as a cutoff to define atrophic cord in that region (i.e., less than the 5th percentile of HC). Subgroup designations were: (1) normal cord size: z > -1.64 in all regional-SCCSA; (2) cervical atrophy only: z ≤ -1.64 in C2–3 and/or C4–5 with z > -1.64 in T4–9; (3) cervical and thoracic atrophy: z ≤ -1.64 in C2–3 and/or C4–5, and T4–9 region; and (4) thoracic atrophy only: z ≤ -1.64 in T4–9 and z > -1.64 in C2–3 and C4–5. Differences in clinical parameters between subgroups within each cohort (RRMS and the combined progressive cohort) were evaluated using one-way ANOVA followed by Tukey's multiple comparisons test. A p-value of<0.005 was considered statistically significant to account for multiple comparisons (two groups, five clinical parameters).

RRMS cases who had multiple scans over the period of the study were divided into two groups for longitudinal analysis based on the change in EDSS between their latest visit and baseline visit. RRMS cases showing clinical progression (progressive-disability group) were defined as those in whom change in EDSS was ≥ 1 if baseline EDSS ≤ 5.5, or change in EDSS ≥ 0.5 if baseline EDSS ≥ 6. (Freeman et al., 2001; Hoogervorst et al., 2003) The files and notes from these cases were also reviewed to confirm that the change in EDSS was due to a chronic progression of disability rather than an acute MS exacerbation. All other cases were grouped as having stable-disability. Characteristics of the two groups at each timepoint (baseline and follow up) were compared using Wilcoxon two-sample test. A random coefficient model for longitudinal data was applied to evaluate the change of regional-SCCSA variables over time, using age at scan as the time variable. The model estimated a random intercept and slope for each patient. The random coefficient model contained disability group (progressive vs. stable), age, and the interaction between disability group and age. An interaction term with p < 0.0167 (corrected for multiple comparisons – three regions) was considered to be statistically significant.

3. Results

The cross-sectional part of this study included 149 RRMS, 49 SPMS, 59 PPMS and 48 HC studied at the NIH over a 6-year period. In addition, follow-up scans were available in 78 RRMS cases over this period, which were included in the longitudinal part of this study. Detailed demographic and clinical information for the cohorts is shown in Table 1.

3.1. Comparison of regional-SCCSA between groups

SCCSA profile plots identified major anatomical regions of the spinal cord in all subgroups, such as cervical enlargement and the transition region between C- and T- spine. The profile plots (Fig. 1A and 1B) were compared and differences between cohorts were observed. Compared to HC, PPMS and SPMS were the most atrophic, with thinning evident throughout the entire length of the cord. However, in RRMS, average cord thinning was found only in the cervical region. Regional-SCCSA measurements in the HC group differed between males and females but were not correlated with age (data not shown). Therefore, sex-adjusted regional-SCCSA data were used for further statistical testing. ANOVA indicated that regional-SCCSA (Fig. 1C) in RRMS was smaller compared to HC in the C2–3 (p = 0.014) and C4–5 (p = 0.002) regions

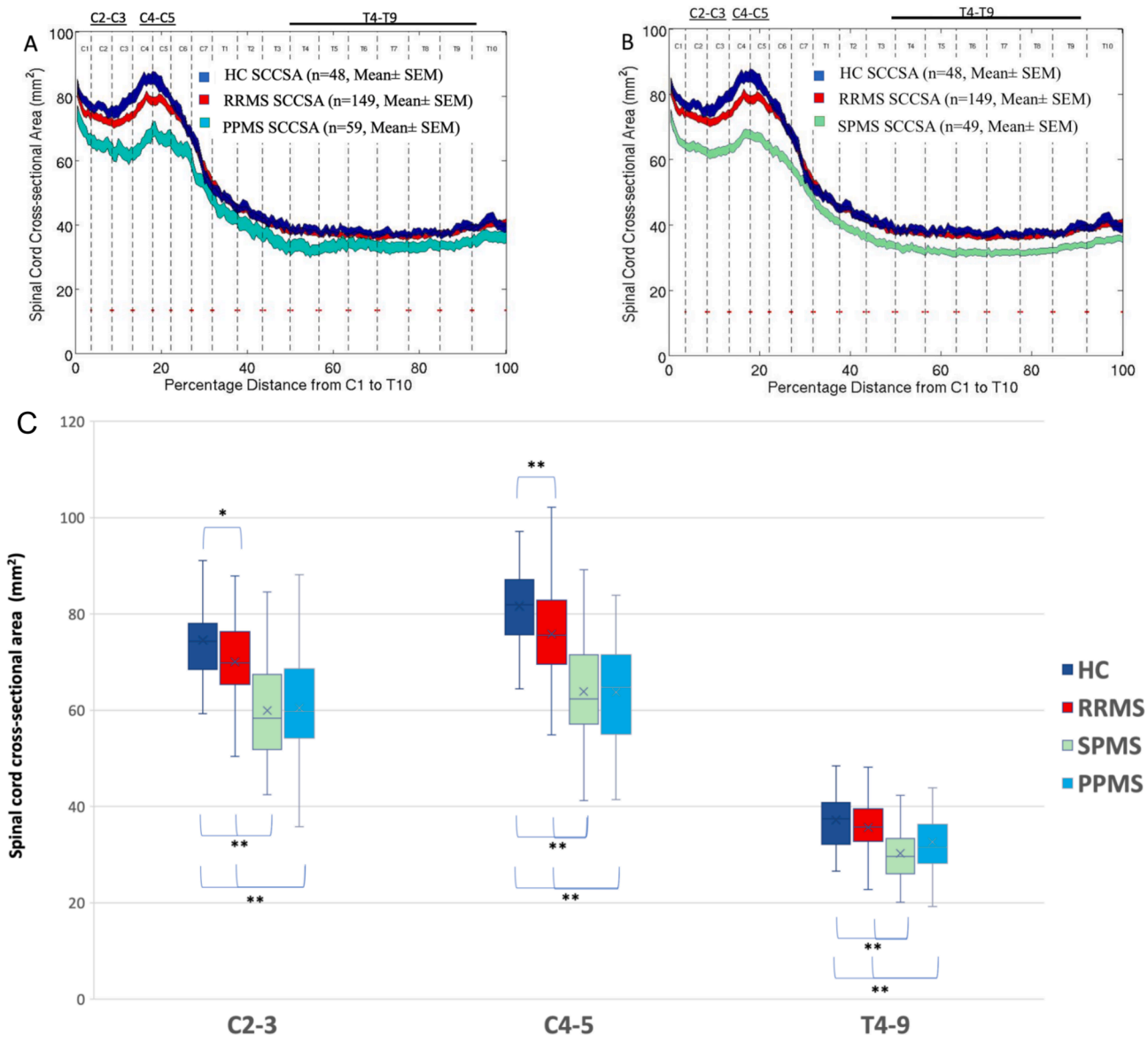

Fig. 1. Comparison of Average SCCSA Profile Plots and Regional-SCCSA Between Cohorts - SCCSA plots between C1–T10 vertebral levels from (A) HC (blue), RRMS (red) and PPMS (teal), and (B) HC (blue), RRMS (red) and SPMS (green) cohorts. Thickness of line indicates standard error of the mean of each cohort. Regional-SCCSA (C) were compared using ANOVA after correcting for sex and Box-Cox data transformation, * $p < 0.0167$, ** $p < 0.005$. Boxes represent quartiles 1 to 3, middle line of the box represents the median, x in the box represents the mean. Whiskers extend between minimum and maximum values. HC: healthy controls, PPMS: primary progressive multiple sclerosis, RRMS: relapsing-remitting multiple sclerosis, SCCSA: spinal cord cross-sectional area, SPMS: secondary progressive multiple sclerosis. (For interpretation of the references to colour in this figure legend, the reader is referred to the web version of this article.)

Table 2
Correlation coefficients of regional-SCCSA (C2–3, C4–5, T4–9) with clinical parameters in multiple sclerosis phenotypes. * $p < 0.0017$, 9-HPT-A: time to complete 9-hole peg test (average of left and right), EDSS: expanded disability status scale, ns: not significant, PPMS: primary progressive multiple sclerosis, RRMS: relapsing-remitting multiple sclerosis, SCCSA – spinal cord cross-sectional area, SNRS: Scripps neurologic rating scale, SPMS: secondary progressive multiple sclerosis, T25FW: timed 25-foot walk.

	Region	Disease duration	EDSS	SNRS	T25FW	9-HPT-A
RRMS	C2-3	−0.44*	−0.30*	0.29*	−0.30*	ns
	C4-5	−0.43*	−0.35*	0.36*	−0.34*	ns
	T4-9	−0.33*	−0.31*	0.32*	−0.32*	ns
SPMS/PPMS	C2-3	ns	−0.39*	0.37*	−0.36*	−0.36*
	C4-5	ns	−0.39*	0.41*	−0.35*	−0.43*
	T4-9	ns	ns	ns	ns	ns

Table 3
Backward regression analysis of clinical parameters using regional-SCCSA for each clinical parameter in the two groups.

ClinicalParameter	RRMS				SPMS/PPMS			
	N	P-value	R^2	Regional-SCCSA kept in the model	N	P-value	R^2	Regional-SCCSA kept in the model
EDSS	129	<0.0001	0.12	C4-5	99	<0.0001	0.18	C2-3
SNRS	123	<0.0001	0.13	C4-5	92	<0.0001	0.18	C4-5
T25FW	122	0.0001	0.12	C4-5	92	0.0003	0.14	C2-3
9-HPT-A	132	0.013	0.05	C4-5	100	0.034	0.22	C4-5 ; T4-9

For each parameter in each group, a model including all 3 regions was created, in which regions with a non-significant impact were removed, until no further regions could be removed without a statistically significant loss of the model fit. Thus, for each parameter the table shows the region(s) with the most significant effect, and these were mostly cervical regions, although the T4-9 region was kept in the model for 9-HPT-A in the progressive cohort.
9-HPT-A: time to complete 9-hole peg test (average of left and right), EDSS: expanded disability status scale, PPMS: primary progressive multiple sclerosis, RRMS: relapsing-remitting multiple sclerosis, SCCSA – spinal cord cross-sectional area, SNRS: Scripps neurologic rating scale, SPMS: secondary progressive multiple sclerosis, T25FW: timed 25-foot walk.

but not in the T4–9 region. In progressive MS (SPMS and PPMS), smaller regional-SCCSA was evident in all regions compared to HC and RRMS ($p < 0.005$). Regional-SCCSA did not differ significantly between SPMS and PPMS.

3.2. Correlation of regional-SCCSA with clinical parameters

In RRMS, correlations were seen between all three regional-SCCSA and all clinical parameters except 9-HPT (Table 2). Analyzing correlation in the progressive cohorts combined (n = 108), cervical regional-SCCSA correlated with all clinical parameters except disease duration, while correlation with the T4–9 region did not meet adjustment for multiple comparisons. In RRMS, the cervical (and thoracic) regional-SCCSA measurements explained about 9–12% of variation in EDSS (max $R^2 = 0.12$, C4–5), SNRS (max $R^2 = 0.13$, C4–5), and T25FW (max $R^2 = 0.12$, C4–5), whereas in the progressive cohorts cervical regional-SCCSA measurements explained 12–18% of variation in EDSS (max $R^2 = 0.15$, C2–3), SNRS (max $R^2 = 0.17$, C4–5), T25FW (max $R^2 = 0.13$, C2–3), and 9-HPT (max $R^2 = 0.18$, C2–3).

Regional-SCCSA measurements were closely correlated in both groups ($p < 0.0001$, minimal $R^2 = 0.5$). The backward elimination regression models for each clinical parameter are presented in Table 3, showing that for most parameters, only one cervical region (C2-3 or C4-5) was kept in the model. However, T4-9 region was kept in the model for 9-HPT in the progressive cohort.

3.3. Comparison of clinical parameters between regional-SCCSA subgroups

Regional-SCCSAs were converted to z-scores based on HC cohort and spinal cord patterns were determined in the different MS cohorts (for details, see Methods). Within the RRMS cohort (Fig. 2A), 78% had normal cord size, whereas 22% had some evidence of spinal cord atrophy. Thoracic atrophy alone was very rare (n = 1, <1%), and the remaining cases of atrophy were distributed between those with evidence of cervical atrophy only (n = 19, 13%) or cervical and thoracic atrophy (n = 13, 9%). By contrast, in progressive MS (Fig. 2A), only around 30% had a normal cord size, whereas 70% had quantifiable evidence of cervical atrophy only or both cervical and thoracic atrophy. Interestingly, the percentage of cases having only cervical atrophy increased from 13% in RRMS to 33% in SPMS. A similar increase from 9% to 34% was seen in percentage of both cervical and thoracic atrophy when comparing these two cohorts.

Within the RRMS cohort, cases with either cervical atrophy or cervical and thoracic atrophy had longer disease duration ($p < 0.0001$) and increased disability as evident by increased EDSS ($p < 0.0002$) and decreased SNRS ($p < 0.004$) compared to cases with normal cord size (Fig. 2B). However, 9-HPT was only different in the cervical and thoracic atrophy subgroup compared to those with a normal cord size ($p < 0.0001$). Within the progressive cohort (SPMS and PPMS combined), EDSS and 9-HPT were higher in the cervical atrophy subgroup compared to cases with normal cord size ($p < 0.005$), whereas SNRS was only lower in the subgroup of cases with both cervical and thoracic atrophy ($p < 0.001$, data not shown).

3.4. Longitudinal regional-SCCSA in RRMS cases

We examined changes in SCSSA over time and their relationship to clinical parameters. In the RRMS cohort, there were 78 individuals with longitudinal clinical and MRI data for analysis (Table 1B). Longitudinal SCCSA profile plots from 2 cases are presented in Fig. 3. A representative case with no clinical progression also showed no change in SCCSA over 32 months (Fig. 3A). On the contrary, a representative case with apparent decrease in SCCSA in various cord regions preceding worsening clinical disability over 30 months period is shown in Fig. 3B.

Of the 78 RRMS with longitudinal scans, 64 had no defined clinical progression of disability between first and last visits (Table 1B). The remaining 14 RRMS had clinical progression as defined by a change in EDSS of 1.0 or more (all had baseline EDSS $\leq$ 5.5) over time (progressive-disability group, Table 1B). Among these 14 individuals, regional-SCCSA from at least one region decreased by more than 2.5% (95% confidence interval test–retest data from our previous study) (Liu et al., 2014) in 10 cases (71%), and C4–5 was the most commonly involved region (9/10 cases). The mixed effects model analysis (Fig. 3C) showed a significant interaction between groups (stable- vs. progressive-disability) and age for cervical regional-SCCSA variables, indicating that the rate of decrease in regional-SCCSA with age in the progressive-disability group was significantly higher than that in the stable-disability group (0.62 mm^2/year vs. 0.07 mm^2/year for C2–3, $p = 0.002$; 0.72 mm^2/year vs. 0.29 mm^2/year for C4–5, $p = 0.004$). Interaction was not significant for the T4–9 region after adjustment for multiple comparisons ($p = 0.038$).

4. Discussion

Our findings show atrophic spinal cord in 22% of RRMS, and in 68% of the progressive MS participants compared to the HC. SCCSA from various regions correlated with most clinical disability scores in all phenotypes, indicating that it is a reliable marker for disease progression in MS. Importantly, thoracic cord atrophy was seen in 10% of RRMS participants, which increased to 35% in SPMS. Preliminary longitudinal analysis showed significantly higher atrophy rates in the cervical cords of participants showing clinical progression than those without clinical progression. These results suggest that SCCSA measured cross-sectionally can be a proxy for cord atrophy, and an objective biomarker for clinical progression.

The RRMS cases studied herein had evidence of cervical cord atrophy compared to HC, supporting similar findings in some studies on the early phases of MS. (Biberacher et al., 2015; Hagström et al., 2017; Brex et al., 2001) However, this is an important observation since some previous studies, (Rocca et al., 2011; Zivadinov et al., 2008) including a large *meta*-analysis (Casserly et al., 2018), have demonstrated this finding in

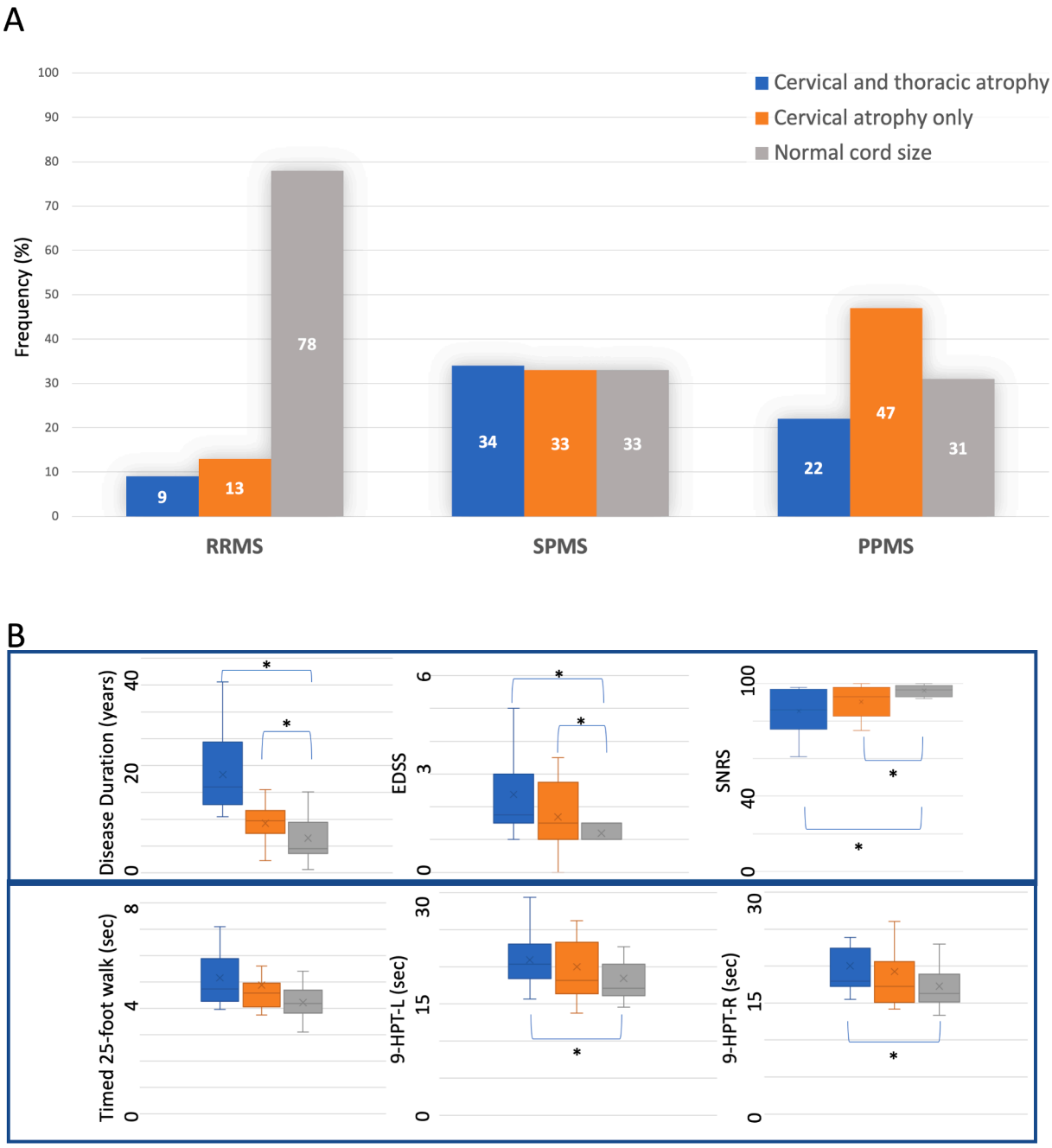

Fig. 2. Frequencies of spinal cord atrophy patterns in different cohorts and comparison of clinical parameters between RRMS subgroups – frequencies of spinal cord atrophy patterns in each cohort (A) showing that the total rate of atrophy increased from 22% in RRMS (13% cervical atrophy only, 9% cervical and thoracic atrophy and < 1% thoracic atrophy only [not shown on graph]) to 67% in SPMS, while comparison of clinical parameters between subgroups within the RRMS cohort (B) shows that cases with spinal cord atrophy had longer disease duration and increased disability, although 9-HPT-L/R was only different in the cervical and thoracic atrophy subgroup when compared to those with normal cord size. Boxes represent quartiles 1 to 3, middle line of the box represents the median, x in the box represents the mean. Whiskers extend between minimum and maximum values. * $p < 0.005$, 9-HPT-L/R: 9-hole peg test left/right, EDSS: expanded disability status scale, PPMS (primary progressive multiple sclerosis), RRMS: relapsing-remitting multiple sclerosis, SNRS: Scripps neurologic rating scale, SPMS (secondary progressive multiple sclerosis), T25FW: timed 25-foot walk.

mixed MS cohorts but not specifically in RRMS. Furthermore, we saw significant correlation between all regional-SCCSA and all clinical measures in the RRMS cohort, and between the cervical regions and most clinical measures in the progressive MS cohorts (Table 2). This finding confirms previous observations of correlation with clinical disability, (Bernitsas et al., 2015; Furby et al., 2008; Oh et al., 2013; Kidd et al., 1996; Evangelou et al., 2005) yet highlights the importance of this correlation specifically earlier in the disease course and contradicts a previous study suggesting correlation with disability was only noted in PPMS. (Tsagkas et al., 2019) One possible explanation for the relatively decreased correlation of the thoracic region in the progressive cohorts could be that there is a lower limit of atrophy in the spinal cord ("floor effect."). It is also a conceivable that there is a limit for detection of atrophy with the imaging technique used in which changes would be more difficult to detect in thinner cords at the same imaging resolution.

Our data also show the highest correlation with clinical disability within the C4–5 region in RRMS, an area with a relatively large amount of gray matter. The backward elimination analysis also showed that this

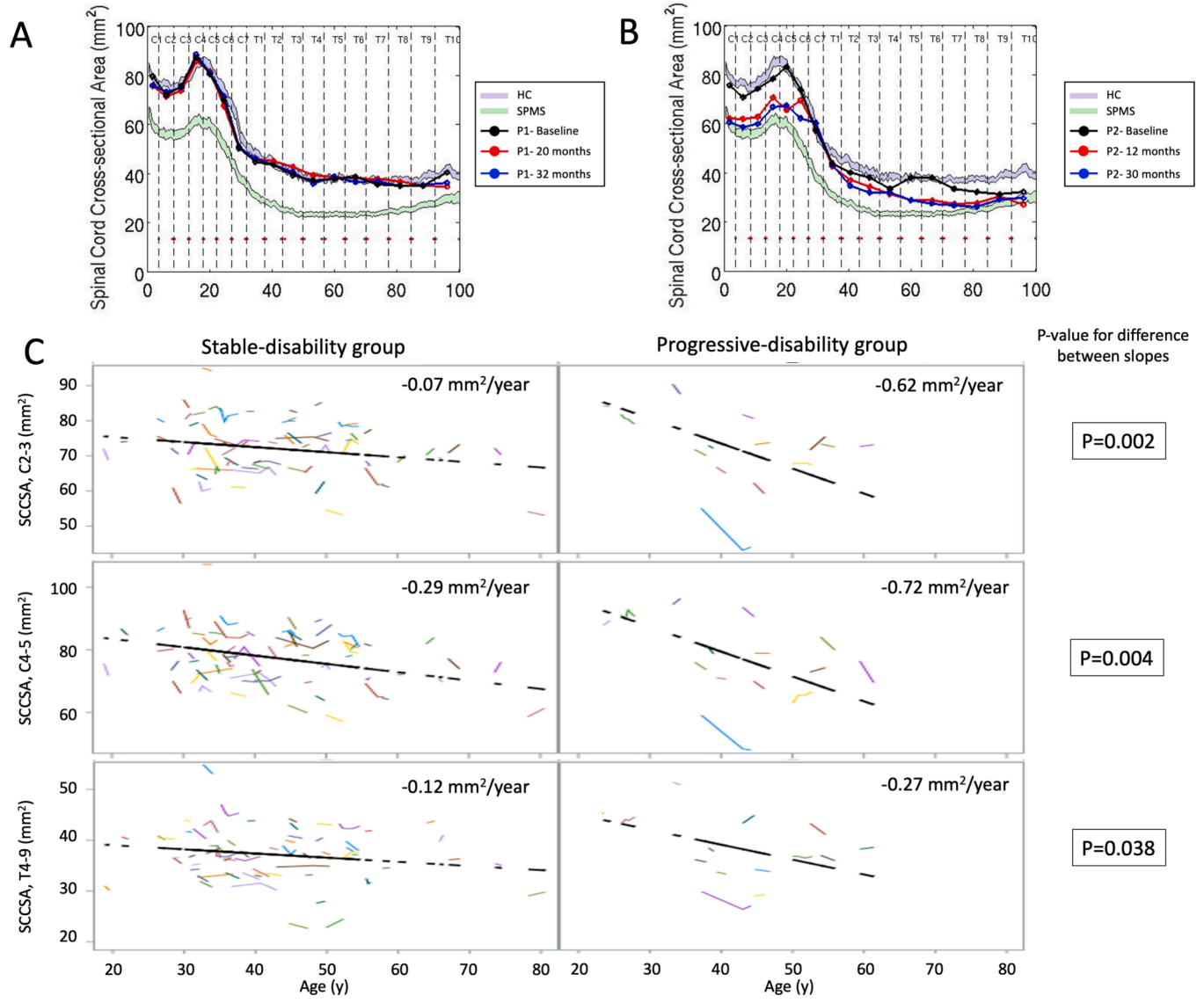

Fig. 3. Longitudinal cohort - representative cases and comparison of change in regional-SCCSA between RRMS cases with stable disability and progressive disability - (A) Longitudinal SCCSA plots derived from a representative individual (a woman with relapsing-remitting multiple sclerosis or RRMS, 39 years old at baseline) scanned at multiple time points (black – baseline, red – 20 months, blue – 32 months), showing no evident change in spinal cord pattern, correlating with no clinical change. (B) Longitudinal SCCSA plots derived from a representative individual (woman with RRMS, 44 years old at baseline) scanned at baseline (black line, EDSS = 0, SNRS = 100), 12 months (red line, EDSS = 0, SNRS = 100), and 30 months (blue line, EDSS = 2, SNRS = 80), showing cord atrophy at the 12-month time point that preceded increased disability at 30 months. This patient had two non-enhancing upper cervical cord lesions that remained unchanged during the entire follow-up. Purple and green lines are averages and standard error of the mean from HC and SPMS respectively, shown here as a reference. (C) Scatter plot showing longitudinal changes in regional SCCSA with age in the relapsing-remitting multiple sclerosis groups (data from each individual is represented by a colored line, top row: C2–3; middle row: C4–5; bottom row: T4–9). Individuals who did not have clinical progression are shown on the left (stable-disability group), and those who had clinical progression are shown on the right (progressive-disability group). The rate of change (mm^2/year) of regional SCCSA was higher in the progressive-disability group cohort compared to the stable-disability group cohort in C2–3 and C4–5 regions, but not in the T4-9 region (p-value presented is for difference in average slope between disability groups and to adjust for multiple comparisons a p-value of <0.0167 was considered to be significant). Black dotted line represents the best fit from the mixed effects model analysis. EDSS: expanded disability status scale, HC: healthy controls, P1: patient 1, P2: patient 2, SCCSA: spinal cord cross-sectional area, SPMS: secondary progressive multiple sclerosis. (For interpretation of the references to colour in this figure legend, the reader is referred to the web version of this article.)

region was most important in the model, and this was also the region with the highest atrophy rate in the longitudinal analysis. While some previous post-mortem studies showed no significant gray matter loss, (Gilmore et al., 2005) we believe that our findings, together with previous studies on gray matter atrophy in the spinal cord, (Schlaeger et al., 2014) warrant further hypothesis testing regarding the important component of neuronal loss in spinal cord atrophy, rather than solely Wallerian degeneration combined with focal demyelination.

Further division of MS cohorts based on radiographic spinal cord patterns suggests that radiological subgrouping might complement clinical characterization. Cervical atrophy was more prevalent than thoracic atrophy in all MS phenotypes, with significant correlation with the various clinical parameters. This suggests the cervical cord as a more attractive target for further evaluation and investigation, especially in the settings of time and resource limitation. However, our data also demonstrate the potential benefits of studying the thoracic spine despite any floor effect, giving a more complete picture of disability and allowing for radiological subgrouping while requiring only a short

addition of time to the type of scans used for our method.

The amount of variability in clinical disability scores explained by regional-SCCSA was relatively modest between 12 and 20%. Certainly, other factors such as tissue damage in the brain and focal lesions in the spinal cord also contribute to disability, but were outside the objective of this study. Interestingly, within the RRMS cohort, the variability explained by the thoracic region was similar to that explained by each of the cervical regions, although the backward elimination analysis demonstrated that the cervical regions are the most important. In addition, most of the RRMS cohort had normal-sized spinal cord and relatively low disability scores, which might have reduced this correlation. Some previous studies showed that specific clinical measures correlate with the corresponding cord area (e.g., lower limb function with the thoracic cord atrophy). (Schlaeger et al., 2015) Our data are consistent to some degree with these observations, as the best correlation with 9-HPT was found in the C4-5 region. However, the majority of the clinical measures did not have good anatomical correlations. Therefore, cord atrophy might be a better reflection of a general neurodegenerative process contributing to overall disability. Additional longitudinal spinal cord studies, combined with brain volume and segmentation analysis, are underway to parse out the contributions of these different effects.

Some prior studies have focused on limiting imaging to a few preselected levels to allow much higher resolution in axial slices. (Schlaeger et al., 2014) However, placing the axial slice exactly perpendicular to the cord in two planes is challenging during image acquisition. We therefore chose to acquire 1-mm isotropic resolution images of the whole cord and compute the perpendicular slices during post-processing, using the edge of the cord as the initial guide, and centroid of the cord for final calculation. This should in principle decrease measurement variability (test–retest intraclass correlation coefficient is 2.5% in our method, as reported previously). (Liu et al., 2014) Nevertheless, increasing the in-plane resolution used in this study might help improve the sensitivity to changes in an already-thin spinal cord, and even remove some of the floor effect seen in thoracic cord.

Collectively, our findings provide support for the concept that there is a subgroup of RRMS where processes of neurodegeneration have already taken place and show that this is more likely in the setting of longer disease duration and higher baseline clinical disability. Whether these patients are at higher risk of developing progressive MS is yet to be determined by further longitudinal studies. The data from our longitudinal analysis in RRMS proves preliminary support for the ability of our technique to track changes in SCCSA, and shows that these changes correlate with — and in some cases even precede — clinical progression. Such considerations may play an important role in optimal patient selection for clinical trials.

While research investigates the underlying drivers of, and possible treatments for, neurodegeneration in MS, (Kawachi and Lassmann, 2017; Friese et al., 2014) it is important to be able to quantitatively measure and track this process, and to determine if clinical interventions impact this aspect of the disease. The techniques presented herein require only a few additional minutes of scanning and can be used to monitor disease progression and correlate with biomarkers that may help further elucidate the mechanisms of atrophy and neurodegeneration. This can affect the way we predict clinical progression and assess effectiveness of disease modifying therapies, and also allow us to create more uniform subpopulations for assessing efficacy of interventions.

The strengths of our study are the research-based use of a consistent MRI protocol, the robust technique allowing mostly automated evaluation of the cervical and thoracic cord requiring only minimal manual input, (Liu et al., 2014) and the large number of participants including a large enough healthy control group for a unique reference-based analysis of atrophy. Limitations of the study include the cross-sectional nature of the main analysis and the lack of data concerning brain and spine lesions, as well as brain volumes, which are possible contributors to disability. However, it is important to recognize that the analysis is focused on the contribution of cord atrophy to disability, and the use of T_1-weighted gradient echo sequence makes the SCCSA measurement insensitive to confounding effects like spinal cord lesions. Another limitation of the study is that only a subgroup of RRMS cases with varying follow-up periods were available for longitudinal analysis. Larger cohorts are currently being recruited in a multi-center study.

In conclusion, we have shown that we can quantify and monitor spinal cord atrophy in various phenotypes of MS. Monitoring cross-sectional changes along the cervical and thoracic cord can help improve the quality of patient care as well as provide a more sensitive marker of disease progression. In addition, radiographic subtyping of RRMS patients using different patterns of atrophy can add to the better clinical monitoring and patient selection for clinical trials.

CRediT authorship contribution statement

Yair Mina: Conceptualization, Methodology, Investigation, Formal analysis, Writing - original draft. **Shila Azodi:** Conceptualization, Methodology, Investigation, Formal analysis, Writing - original draft. **Tsemacha Dubuche:** Formal analysis, Investigation. **Frances Andrada:** Investigation, Resources. **Ikesinachi Osuorah:** Investigation, Resources. **Joan Ohayon:** Investigation, Resources. **Irene Cortese:** Conceptualization, Investigation, Resources. **Tianxia Wu:** Formal analysis, Data curation. **Kory R. Johnson:** Formal analysis, Data curation. **Daniel S. Reich:** Conceptualization, Investigation, Writing - review & editing. **Govind Nair:** Conceptualization, Methodology, Software, Formal analysis, Writing - review & editing. **Steven Jacobson:** Conceptualization, Methodology, Writing - review & editing.

Declaration of Competing Interest

The authors declare that they have no known competing financial interests or personal relationships that could have appeared to influence the work reported in this paper.

Acknowledgements

We thank the staff at the Neuroimmunology Clinic and the Functional Magnetic Resonance Imaging Facility at the NIH. Study funded by the Intramural Research Program at the National Institute of Neurological Disorders and Stroke.

References

Longo, D.L., Reich, D.S., Lucchinetti, C.F., Calabresi, P.A., 2018. Multiple Sclerosis. N. Engl. J. Med. 378 (2), 169–180.

Lublin, F.D., Reingold, S.C., Cohen, J.A., et al., 2014. Defining the clinical course of multiple sclerosis. Neurology. 83 (3), 278.

Sastre-Garriga, J., Pareto, D., Battaglini, M., Rocca, M.A., Ciccarelli, O., Enzinger, C., Wuerfel, J., Sormani, M.P., Barkhof, F., Yousry, T.A., De Stefano, N., Tintoré, M., Filippi, M., Gasperini, C., Kappos, L., Río, J., Frederiksen, J., Palace, J., Vrenken, H., Montalban, X., Rovira, À., 2020. MAGNIMS consensus recommendations on the use of brain and spinal cord atrophy measures in clinical practice. Nature Reviews Neurology. 16 (3), 171–182.

Losseff, N.A., Webb, S.L., O'Riordan, J.I., Page, R., Wang, L., Barker, G.J., Tofts, P.S., McDonald, W.I., Miller, D.H., Thompson, A.J., 1996. Spinal cord atrophy and disability in multiple sclerosis. A new reproducible and sensitive MRI method with potential to monitor disease progression. Brain. 119 (3), 701–708.

Horsfield, M.A., Filippi, M., 2003. Spinal cord atrophy and disability in multiple sclerosis over four years. J Neurol Neurosurg Psychiatry. 74 (8), 1014–1015.

M. Moccia S. Ruggieri A. Ianniello A. Toosy C. Pozzilli O. Ciccarelli Advances in spinal cord imaging in multiple sclerosis Ther Adv Neurol Disord. 12 2019 175628641984059 10.1177/1756286419840593.

Zurawski, J., Glanz, B.I., Healy, B.C., Tauhid, S., Khalid, F., Chitnis, T., Weiner, H.L., Bakshi, R., 2019. The impact of cervical spinal cord atrophy on quality of life in multiple sclerosis. J Neurol Sci. 403, 38–43.

Casserly, C., Seyman, E.E., Alcaide-Leon, P., Guenette, M., Lyons, C., Sankar, S., Svendrovski, A., Baral, S., Oh, J., 2018. Spinal Cord Atrophy in Multiple Sclerosis: A Systematic Review and Meta-Analysis. J Neuroimaging. 28 (6), 556–586.

Bot, J.C.J., Barkhof, F., Polman, C.H., Nijeholt, G.J.L.a., de Groot, V., Bergers, E., Ader, H.J., Castelijns, J.A., 2004. Spinal cord abnormalities in recently diagnosed MS patients: added value of spinal MRI examination. Neurology. 62 (2), 226–233.

Azodi, S., Nair, G., Enose-Akahata, Y., Charlip, E., Vellucci, A., Cortese, I., Dwyer, J., Billioux, B.J., Thomas, C., Ohayon, J., Reich, D.S., Jacobson, S., 2017. Imaging spinal cord atrophy in progressive myelopathies: HTLV-I-associated neurological disease (HAM/TSP) and multiple sclerosis (MS). Ann Neurol. 82 (5), 719–728.

Ciccarelli, O., Cohen, J.A., Reingold, S.C., Weinshenker, B.G., Amato, M.P., Banwell, B., Barkhof, F., Bebo, B., Becher, B., Bethoux, F., Brandt, A., Brownlee, W., Calabresi, P., Chatway, J., Chien, C., Chitnis, T., Ciccarelli, O., Cohen, J., Comi, G., Correale, J., De Sèze, J., De Stefano, N., Fazekas, F., Flanagan, E., Freedman, M., Fujihara, K., Galetta, S., Goldman, M., Greenberg, B., Hartung, H.-P., Hemmer, B., Henning, A., Izbudak, I., Kappos, L., Lassmann, H., Laule, C., Levy, M., Lublin, F., Lucchinetti, C., Lukas, C., Marrie, R.A., Miller, A., Miller, D., Montalban, X., Mowry, E., Ourselin, S., Paul, F., Pelletier, D., Ranjeva, J.-P., Reich, D., Reingold, S., Rocca, M.A., Rovira, A., Schlaerger, R., Soelberg Sorensen, P., Sormani, M., Stuve, O., Thompson, A., Tintoré, M., Traboulsee, A., Trapp, B., Trojano, M., Uitdehaag, B., Vukusic, S., Waubant, E., Weinshenker, B., Wheeler-Kingshott, C.G., Xu, J., 2019. Spinal cord involvement in multiple sclerosis and neuromyelitis optica spectrum disorders. The Lancet Neurology. 18 (2), 185–197.

Aymerich, F.X., Auger, C., Alonso, J., Alberich, M., Sastre-Garriga, J., Tintoré, M., Montalban, X., Rovira, A., 2018. Cervical Cord Atrophy and Long-Term Disease Progression in Patients with Primary-Progressive Multiple Sclerosis. American Journal of Neuroradiology. 39 (2), 399–404.

Bonati, U., Fisniku, L.K., Altmann, D.R., Yiannakas, M.C., Furby, J., Thompson, A.J., Miller, D.H., Chard, D.T., 2011. Cervical cord and brain grey matter atrophy independently associate with long-term MS disability. J Neurol Neurosurg Psychiatry. 82 (4), 471–472.

Bjartmar, C., Kidd, G., Mork, S., Rudick, R., Trapp, B.D., 2000. Neurological disability correlates with spinal cord axonal loss and reduced N-acetyl aspartate in chronic multiple sclerosis patients. Ann Neurol. 48 (6), 893–901.

Song, X., Li, D., Qiu, Z., Su, S., Wu, Y., Wang, J., Liu, Z., Dong, H., 2020. Correlation between EDSS scores and cervical spinal cord atrophy at 3T MRI in multiple sclerosis: A systematic review and meta-analysis. Multiple Sclerosis and Related Disorders. 37, 101426. https://doi.org/10.1016/j.msard.2019.101426.

Daams, M., Steenwijk, M.D., Wattjes, M.P., Geurts, J.J.G., Uitdehaag, B.M.J., Tewarie, P. K., Balk, L.J., Pouwels, P.J.W., Killestein, J., Barkhof, F., 2015. Unraveling the neuroimaging predictors for motor dysfunction in long-standing multiple sclerosis. Neurology. 85 (3), 248–255.

A.B. Cohen M. Neema A. Arora E. Dell'Oglio R.H.B. Benedict S. Tauhid D. Goldberg-Zimring C. Chavarro-Nieto A. Ceccarelli J.P. Klein J.M. Stankiewicz M.K. Houtchens G.J. Buckle D.C. Alsop C.R.G. Guttmann R. Bakshi The relationships among MRI-defined spinal cord involvement, brain involvement, and disability in multiple sclerosis 22 2 2012 122 128.

Ukkonen, M., Dastidar, P., Heinonen, T., Laasonen, E., Elovaara, I., 2003. Volumetric quantitation by MRI in primary progressive multiple sclerosis: volumes of plaques and atrophy correlated with neurological disability. Eur J Neurol. 10 (6), 663–669.

Oh, J., Sotirchos, E.S., Saidha, S., Whetstone, A., Chen, M., Newsome, S.D., Zackowski, K., Balcer, L.J., Frohman, E., Prince, J., Diener-West, M., Reich, D.S., Calabresi, P.A., 2015. Relationships between quantitative spinal cord MRI and retinal layers in multiple sclerosis. Neurology. 84 (7), 720–728.

Andelova, M., Uher, T., Krasensky, J., Sobisek, L., Kusova, E., Srpova, B., Vodehnalova, K., Friedova, L., Motyl, J., Preiningerova, J.L., Kubala Havrdova, E., Horakova, D., Vaneckova, M., 2019. Additive Effect of Spinal Cord Volume, Diffuse and Focal Cord Pathology on Disability in Multiple Sclerosis. Front Neurol. 10 https://doi.org/10.3389/fneur.2019.00820.

Tsagkas, C., Magon, S., Gaetano, L., Pezold, S., Naegelin, Y., Amann, M., Stippich, C., Cattin, P., Wuerfel, J., Bieri, O., Sprenger, T., Kappos, L., Parmar, K., 2018. Spinal cord volume loss: A marker of disease progression in multiple sclerosis. Neurology. 91 (4), e349–e358.

Lukas, C., Knol, D.L., Sombekke, M.H., Bellenberg, B., Hahn, H.K., Popescu, V., Weier, K., Radue, E.W., Gass, A., Kappos, L., Naegelin, Y., Uitdehaag, B.M.J., Geurts, J.J.G., Barkhof, F., Vrenken, H., 2015. Cervical spinal cord volume loss is related to clinical disability progression in multiple sclerosis. J Neurol Neurosurg Psychiatry. 86 (4), 410–418.

Stevenson, V.L., Leary, S.M., Losseff, N.A., Parker, G.J.M., Barker, G.J., Husmani, Y., Miller, D.H., Thompson, A.J., 1998. Spinal cord atrophy and disability in MS: a longitudinal study. Neurology. 51 (1), 234–238.

Bernitsas, E., Bao, F., Seraji-Bozorgzad, N., Chorostecki, J., Santiago, C., Tselis, A., Caon, C., Zak, I., Millis, S., Khan, O., 2015. Spinal cord atrophy in multiple sclerosis and relationship with disability across clinical phenotypes. Multiple Sclerosis and Related Disorders. 4 (1), 47–51.

Rocca, M.A., Valsasina, P., Meani, A., et al., 2019. Clinically relevant cranio-caudal patterns of cervical cord atrophy evolution in MS. Neurology. 93 (20), e1852.

Rocca, M.A., Horsfield, M.A., Sala, S., Copetti, M., Valsasina, P., Mesaros, S., Martinelli, V., Caputo, D., Stosic-Opincal, T., Drulovic, J., Comi, G., Filippi, M., 2011. A multicenter assessment of cervical cord atrophy among MS clinical phenotypes. Neurology. 76 (24), 2096–2102.

Bieniek, M., Altmann, D.R., Davies, G.R., et al., 2006. Cord atrophy separates early primary progressive and relapsing remitting multiple sclerosis. J. Neurol. Neurosurg. Psychiatry 77 (9), 1036–1039.

Schlaeger, R., Papinutto, N., Zhu, A.H., Lobach, I.V., Bevan, C.J., Bucci, M., Castellano, A., Gelfand, J.M., Graves, J.S., Green, A.J., Jordan, K.M., Keshavan, A., Panara, V., Stern, W.A., von Büdingen, H.-C., Waubant, E., Goodin, D.S., Cree, B.A. C., Hauser, S.L., Henry, R.G., 2015. Association Between Thoracic Spinal Cord Gray Matter Atrophy and Disability in Multiple Sclerosis. JAMA Neurol. 72 (8), 897. https://doi.org/10.1001/jamaneurol.2015.0993.

Klein, J.P., Arora, A., Neema, M., Healy, B.C., Tauhid, S., Goldberg-Zimring, D., Chavarro-Nieto, C., Stankiewicz, J.M., Cohen, A.B., Buckle, G.J., Houtchens, M.K., Ceccarelli, A., Dell'Oglio, E., Guttmann, C.R.G., Alsop, D.C., Hackney, D.B., Bakshi, R., 2011. A 3T MR imaging investigation of the topography of whole spinal cord atrophy in multiple sclerosis. AJNR Am J Neuroradiol. 32 (6), 1138–1142.

Leary, S.M., Miller, D.H., Stevenson, V.L., Brex, P.A., Chard, D.T., Thompson, A.J., 2003. Interferon β-1a in primary progressive MS. Neurology. 60 (1), 44.

Lin, X., Tench, C.R., Turner, B., Blumhardt, L.D., Constantinescu, C.S., 2003. Spinal cord atrophy and disability in multiple sclerosis over four years: application of a reproducible automated technique in monitoring disease progression in a cohort of the interferon β-1a (Rebif) treatment trial. J. Neurol. Neurosurg. Psychiatry 74 (8), 1090.

Kapoor, R., Furby, J., Hayton, T., Smith, K.J., Altmann, D.R., Brenner, R., Chataway, J., Hughes, R.AC., Miller, D.H., 2010. Lamotrigine for neuroprotection in secondary progressive multiple sclerosis: a randomised, double-blind, placebo-controlled, parallel-group trial. The Lancet Neurology. 9 (7), 681–688.

Tur, C., Moccia, M., Barkhof, F., Chataway, J., Sastre-Garriga, J., Thompson, A.J., Ciccarelli, O., 2018. Assessing treatment outcomes in multiple sclerosis trials and in the clinical setting. Nature Reviews Neurology. 14 (2), 75–93.

Daams, M., Weiler, F., Steenwijk, M.D., Hahn, H.K., Geurts, J.JG., Vrenken, H., van Schijndel, R.A., Balk, L.J., Tewarie, P.K., Tillema, J.-M., Killestein, J., Uitdehaag, B. MJ., Barkhof, F., 2014. Mean upper cervical cord area (MUCCA) measurement in long-standing multiple sclerosis: relation to brain findings and clinical disability. Mult Scler. 20 (14), 1860–1865.

De Leener, B., Lévy, S., Dupont, S.M., Fonov, V.S., Stikov, N., Louis Collins, D., Callot, V., Cohen-Adad, J., 2017. SCT: Spinal Cord Toolbox, an open-source software for processing spinal cord MRI data. Neuroimage. 145, 24–43.

Liu, W., Nair, G., Vuolo, L., Bakshi, A., Massoud, R., Reich, D.S., Jacobson, S., 2014. In vivo imaging of spinal cord atrophy in neuroinflammatory diseases. Ann Neurol. 76 (3), 370–378.

Prados, F., Moccia, M., Johnson, A., Yiannakas, M., Grussu, F., Cardoso, M.J., Ciccarelli, O., Ourselin, S., Barkhof, F., Wheeler-Kingshott, C., 2020. Generalised boundary shift integral for longitudinal assessment of spinal cord atrophy. NeuroImage. 209, 116489. https://doi.org/10.1016/j.neuroimage.2019.116489.

D.B. McCoy S.M. Dupont C. Gros J. Cohen-Adad R.J. Huie A. Ferguson X. Duong-Fernandez L.H. Thomas V. Singh J. Narvid L. Pascual N. Kyritsis M.S. Beattie J.C. Bresnahan S. Dhall W. Whetstone J.F. Talbott Convolutional Neural Network-Based Automated Segmentation of the Spinal Cord and Contusion Injury: Deep Learning Biomarker Correlates of Motor Impairment in Acute Spinal Cord Injury 10.3174/ajnr.A6020.

Freeman, J.A., Thompson, A.J., Fitzpatrick, R., et al., 2001. Interferon-β1b in the treatment of secondary progressive MS. Neurology. 57 (10), 1870.

Hoogervorst, E.L.J., Eikelenboom, M.J., Uitdehaag, B.M.J., Polman, C.H., 2003. One year changes in disability in multiple sclerosis: neurological examination compared with patient self report. J Neurol Neurosurg Psychiatry. 74 (4), 439–442.

Biberacher, V., Boucard, C.C., Schmidt, P., Engl, C., Buck, D., Berthele, A., Hoshi, M.-M., Zimmer, C., Hemmer, B., Mühlau, M., 2015. Atrophy and structural variability of the upper cervical cord in early multiple sclerosis. Mult Scler. 21 (7), 875–884.

Hagström, I.T., Schneider, R., Bellenberg, B., Salmen, A., Weiler, F., Köster, O., Gold, R., Lukas, C., 2017. Relevance of early cervical cord volume loss in the disease evolution of clinically isolated syndrome and early multiple sclerosis: a 2-year follow-up study. J Neurol. 264 (7), 1402–1412.

Brex, P.A., Leary, S.M., O'Riordan, J.I., et al., 2001. Measurement of spinal cord area in clinically isolated syndromes suggestive of multiple sclerosis. J Neurol Neurosurg Psychiatry. 70 (4), 544–547.

Zivadinov, R., Banas, A.C., Yella, V., Abdelrahman, N., Weinstock-Guttman, B., Dwyer, M.G., 2008. Comparison of Three Different Methods for Measurement of Cervical Cord Atrophy in Multiple Sclerosis. American Journal of Neuroradiology. 29 (2), 319–325.

Furby, J., Hayton, T., Anderson, V., Altmann, D., Brenner, R., Chataway, J., Hughes, RAC, Smith, K.J., Miller, D.H., Kapoor, R., 2008. Magnetic resonance imaging measures of brain and spinal cord atrophy correlate with clinical impairment in secondary progressive multiple sclerosis. Multiple Sclerosis Journal. 14 (8), 1068–1075.

Oh, J., Saidha, S., Chen, M., Smith, S.A., Prince, J., Jones, C., Diener-West, M., van Zijl, P. C.M., Reich, D.S., Calabresi, P.A., 2013. Spinal cord quantitative MRI discriminates between disability levels in multiple sclerosis. Neurology. 80 (6), 540–547.

Kidd, D., Thorpe, J.W., Kendall, B.E., Barker, G.J., Miller, D.H., McDonald, W.I., Thompson, A.J., 1996. MRI dynamics of brain and spinal cord in progressive multiple sclerosis. J. Neurol. Neurosurg. Psychiatry 60 (1), 15–19.

Evangelou, N., DeLuca, G.C., Owens, T., Esiri, M.M., 2005. Pathological study of spinal cord atrophy in multiple sclerosis suggests limited role of local lesions. Brain. 128 (1), 29–34.

Tsagkas, C., Magon, S., Gaetano, L., Pezold, S., Naegelin, Y., Amann, M., Stippich, C., Cattin, P., Wuerfel, J., Bieri, O., Sprenger, T., Kappos, L., Parmar, K., 2019. Preferential spinal cord volume loss in primary progressive multiple sclerosis. Mult Scler. 25 (7), 947–957.

Gilmore, C.P., DeLuca, G.C., Bö, L., Owens, T., Lowe, J., Esiri, M.M., Evangelou, N., 2005. Spinal Cord Atrophy in Multiple Sclerosis Caused by White Matter Volume Loss. Arch. Neurol. 62 (12), 1859. https://doi.org/10.1001/archneur.62.12.1859.

Schlaeger, R., Papinutto, N., Panara, V., Bevan, C., Lobach, I.V., Bucci, M., Caverzasi, E., Gelfand, J.M., Green, A.J., Jordan, K.M., Stern, W.A., von Büdingen, H.-C., Waubant, E., Zhu, A.H., Goodin, D.S., Cree, B.A.C., Hauser, S.L., Henry, R.G., 2014. Spinal cord gray matter atrophy correlates with multiple sclerosis disability. Ann Neurol. 76 (4), 568–580.

Kawachi, I., Lassmann, H., 2017. Neurodegeneration in multiple sclerosis and neuromyelitis optica. J. Neurol. Neurosurg. Psychiatry 88 (2), 137–145.

Friese, M.A., Schattling, B., Fugger, L., 2014. Mechanisms of neurodegeneration and axonal dysfunction in multiple sclerosis. Nature Reviews Neurology. 10 (4), 225–238.